

# Structural Model of the Ubch5B/CNOT4 Complex Revealed by Combining NMR, Mutagenesis, and Docking Approaches

Cyril Dominguez,<sup>1</sup> Alexandre M.J.J. Bonvin,<sup>1</sup>  
G. Sebastiaan Winkler,<sup>2</sup> Frederik M.A. van Schaik,<sup>2</sup>  
H.Th. Marc Timmers,<sup>2</sup> and Rolf Boelens<sup>1,\*</sup>

<sup>1</sup>Department of NMR Spectroscopy  
Bijvoet Center for Biomolecular Research  
Utrecht University  
Padualaan 8  
3584 Utrecht

<sup>2</sup>Department of Physiological Chemistry  
University Medical Center Utrecht  
Universiteitsweg 100  
3584 CG Utrecht  
The Netherlands

## Summary

The protein CNOT4 possesses an N-terminal RING finger domain that acts as an E3 ubiquitin ligase and specifically interacts with Ubch5B, a ubiquitin-conjugating enzyme. The structure of the CNOT4 RING domain has been solved and the amino acids important for the binding to Ubch5B have been mapped. Here, the residues of Ubch5B important for the binding to CNOT4 RING domain were identified by NMR chemical shift perturbation experiments, and these data were used to generate structural models of the complex with the program HADDOCK. Together with the NMR data, additional biochemical data were included in a second docking, and comparisons of the resulting model with the structure of the c-Cbl/UbcH7 complex reveal some significant differences, notably at specific residues, and give structural insights into the E2/E3 specificity.

## Introduction

The RING finger protein CNOT4 is a component of the CCR4-NOT complex, a global repressor of RNA polymerase II transcription (Collart, 2003; Denis and Chen, 2003). The structure of the RING finger domain of CNOT4, consisting of the 78 N-terminal residues has been solved by NMR (Hanzawa et al., 2001). Recently, CNOT4 has been identified as an E3 ubiquitin-protein ligase, and the RING domain of CNOT4 has been shown to be necessary and sufficient to specifically interact with the ubiquitin-conjugating enzyme, Ubch5B (Albert et al., 2002). These results link CCR4-NOT-mediated transcription repression with the ubiquitination pathway. Whether this ubiquitination is related to degradation of transcription complexes by the 26S proteasome or other regulatory functions is unclear.

Ubiquitination of a substrate involves three enzymes: a ubiquitin-activating enzyme (E1), a ubiquitin-conjugating enzyme (E2) and, finally, a ubiquitin-protein ligase (E3) (Glickman and Ciechanover, 2002; Pickart, 2001;

Weissman, 2001). Different classes of E3 ligases have been found that mediate substrate ubiquitination. E3 enzymes can be distinguished by their E2-interacting domains, which include the HECT and the RING domains (Glickman and Ciechanover, 2002; Pickart, 2001). Therefore, specific E2/E3 pairs are thought to be responsible for mediating target recognition and subsequent ubiquitination. Structures of nine E2 enzymes from different species in the free form have been solved by X-ray crystallography (Cook et al., 1992, 1993, 1997; Hamilton et al., 2001; Jiang and Basavappa, 1999; Lin et al., 2002; Tong et al., 1997; VanDemark et al., 2001; Worthylake et al., 1998) and one was solved by NMR (Miura et al., 2002). The structure of the human E2 enzyme Ubch5B, however, has not been determined. Furthermore, five structures of E2 in complex with various other proteins have been solved by X-ray crystallography (Bernier-Villamor et al., 2002; Huang et al., 1999; Moraes et al., 2001; VanDemark et al., 2001; Zheng et al., 2000). All structures possess the same fold corresponding to an N-terminal  $\alpha$  helix, followed by a four-stranded antiparallel  $\beta$  sheet and three  $\alpha$  helices. The ternary fold is well conserved among the structures both in free form and in complex with other proteins.

Among the E2 structures in complex, two are of particular interest for the E2/E3 recognition: the X-ray structures of the ubiquitin-conjugating enzyme Ubch7 in complex with the E6AP ubiquitin ligase (Huang et al., 1999) and of Ubch7 in complex with the c-Cbl ubiquitin ligase (Zheng et al., 2000). E6AP contains a HECT domain and c-Cbl possesses a C-terminal RING finger domain. Both domains are responsible for the interaction with Ubch7. Besides the RING finger domain of c-Cbl, a second domain, the so-called linker region, also makes contacts with Ubch7. The two structures give considerable insights into the molecular basis of the E2/E3 recognition. Although the RING domain of c-Cbl and the HECT domain of E6AP are structurally unrelated, they both bind Ubch7 in a very similar manner. In both complexes, the same residues of Ubch7 are involved in the interaction and these residues are highly conserved within the E2 enzymes suggesting that other E2/E3 complexes could follow a similar arrangement. There are a limited number of E2 enzymes (13 in *Saccharomyces cerevisiae* and more in higher organisms) whereas the number of E3 protein ligases is still increasing (more than 350 RING domains have been identified in human). This suggests that one E2 can recognize different E3s and that one E3 will only recognize one or few E2s. Correspondingly, it has been shown that the E2/E3 interaction is highly specific; for example, the RING domain of CNOT4 interacts functionally with Ubch5B but not with several other E2 enzymes (Winkler et al., 2004). Similarly, it has recently been shown that the RING protein BRCA1 can interact both with Ubch5C and Ubch7 but that only Ubch5C is functional in BRCA1-mediated substrate-independent Ub-ligase assay (Brzovic et al., 2003). The c-Cbl/UbcH7 and Ubch7/E6-AP complexes involving the same E2 enzyme are thus not sufficient to

\*Correspondence: r.boelens@chem.uu.nl

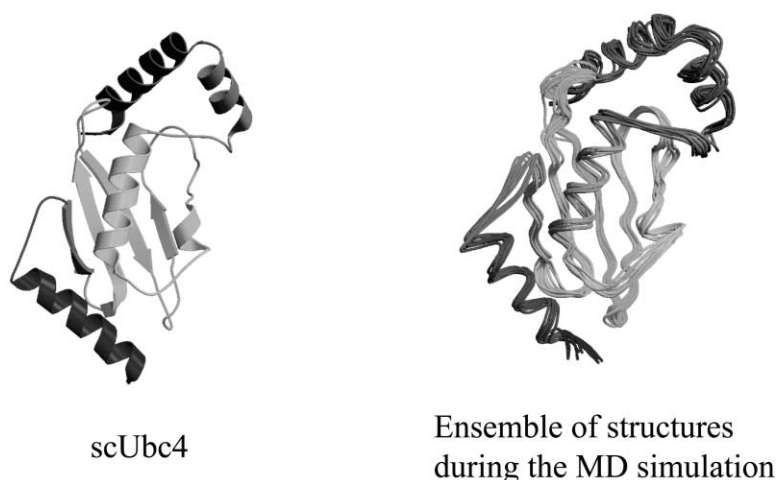


Figure 1. X-Ray Structure of Yeast Ubc4 and Ensemble of Ubch5B Models during the 5 ns Molecular Dynamic Simulation

Figures were generated with the programs Molscript (Kraulis, 1991) and Raster3D (Merrit and Murphy, 1994).

understand the molecular basis of the E2/E3 specificity and structural information from complexes involving other ubiquitin-conjugating enzymes is crucial to understand the E2/E3 specificity at a molecular level.

It has been previously reported that the CNOT4 RING finger domain interacts with Ubch5B, and the amino acids of CNOT4 important for the binding to Ubch5B have been determined by NMR (Albert et al., 2002). Now, we performed the complementary NMR titration experiments to identify the amino acids of Ubch5B that are involved in the binding to the CNOT4 RING finger domain. Using data from the two titrations, we applied a docking approach HADDOCK (Dominguez et al., 2003), which we have recently developed, to generate a structural model of the Ubch5B/CNOT4 RING complex. The initial docking calculations resulted in two possible models of the Ubch5B/CNOT4 complex. Additional biochemical information (Winkler et al., 2004) was used together with the NMR titration restraints in a second docking calculation resulting in a uniquely defined complex. Our final experimentally based model of the Ubch5B/CNOT4 complex reveals significant differences in terms of intermolecular contacts as compared to the c-Cbl/UbcH7 complex, especially in terms of hydrogen bonding and salt bridges. These differences indicate that, although similar and well-conserved regions of different E2 enzymes and E3 ligases are involved in binding, the intermolecular interactions involve different amino acids and different kinds of forces that can explain the observed E2/E3 specificity of the Ubch5B/CNOT4 complex.

## Results and Discussion

### Assignment of Ubch5B and Secondary Structure Prediction

The assignment of Ubch5B was previously reported (Farrow et al., 2000). However, the data were collected at different temperature, pH, and salt concentration than used here. Therefore, 3D TOCSY- $(^1\text{H}, ^{15}\text{N})$  HSQC, 3D NOESY- $(^1\text{H}, ^{15}\text{N})$  HSQC, 3D HNCACB, and 3D CBCA-CONH were recorded to assign the backbone chemical shifts in our conditions (300 K, pH 7.0, 150 mM KCl). Side chain protons were assigned from 3D  $(\text{H})\text{CCH}$

TOCSY and  $\text{H}(\text{C})\text{CH}$  TOCSY experiments. Talos (Cornilescu et al., 1999) was used to predict the dihedral angles of the protein based on the  $\text{C}\alpha$  and the  $\text{C}\beta$  chemical shifts. These predictions correlate well with the consensus secondary structure elements found in the known E2 structures (data not shown).

### Structural Model of Ubch5B

Although the structure of Ubch5B is not available in the Protein Data Bank (PDB), the amino acid sequence of Ubch5B is highly homologous to that of other E2 enzymes. All E2 structures already described are structurally very similar, and our secondary structure prediction based on the NMR  $\text{C}\alpha$  and  $\text{C}\beta$  chemical shifts of Ubch5B correlates well with the E2 consensus structure. We therefore decided to generate a structural model of Ubch5B based on homologous structures. A Blast search of the Ubch5B sequence against the Protein Data Bank identified the most homologous E2 enzymes. In particular, Ubch5B displays 90% homology and 80% identity with yeast Ubc4 (PDB: 1QCQ). Therefore, yeast Ubc4 was used to build a homology model of Ubch5B. The Ramachandran plot of the generated model shows 89.8% of the residues in the most favored regions, 9.5% in the additional allowed regions, 0.6% in the generously allowed region, and 0.2% in the disallowed regions. The backbone rmsd between the model and the yeast Ubc4 structure is 0.20 Å. A 5 ns molecular dynamic simulation in explicit solvent was performed in order to assess the stability of the model and to obtain an ensemble of starting structures for the docking by extracting PDB files from the trajectory (see Experimental Procedures). Analysis of these PDB files shows that few structural rearrangements occur during the simulation. The mean rmsd among all structures extracted from the trajectory is 1.2 Å for the backbone atoms (Figure 1) and 1.7 Å for all heavy atoms.

### Mapping of the CNOT4-N78 Binding Site of Ubch5B

The Ubch5B binding site of the CNOT4 RING domain has been previously determined by NMR chemical shift perturbations in a titration of  $^{15}\text{N}$ -labeled CNOT4-N78 (comprising the 78 N-terminal amino acids of CNOT4)

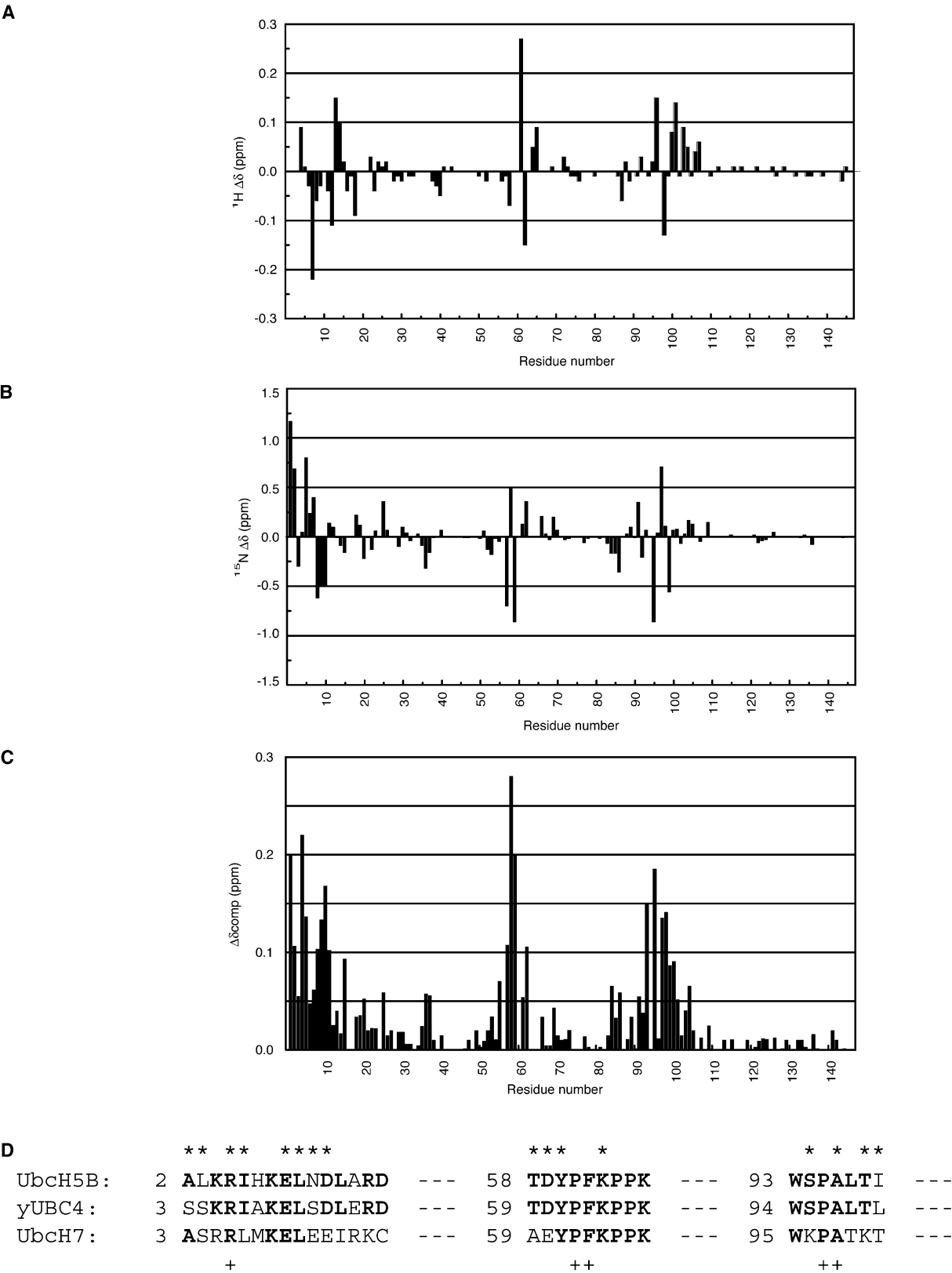


Figure 2. Titration of CNOT4 with Ubch5B  
(A and B) Chemical shifts perturbation of  $^{15}\text{N}$ -labeled Ubch5B upon titration of CNOT4-N78 as a function of the Ubch5B amino acid for the (A) amide proton and (B) the amide nitrogen.  
(C) Combined chemical shift differences ( $\Delta\delta = [(\delta_{\text{HN}})^2 + (\delta_{\text{N}}/6.51)^2]^{1/2}$ ).  
(D) Sequence alignment of Ubch5B, yeast UBC4, and Ubch7 encompassing the  $\alpha 1$  helix and the L1 and L2 loops. The amino acids of Ubch5B displaying a  $\Delta\delta_{\text{comp}} > 0.1$  ppm (\*), and the amino acids of Ubch7 involved in the binding with c-Cbl (+) are marked.

Table 1. Performance of Ensemble Docking with HADDOCK for EIIA-HPr Complex

	Original Protocol	Ensemble Docking	NMR Structure
Backbone rmsd from NMR structure (Å)	2.5 ± 0.2	1.4 ± 0.2	—
Backbone interface rmsd from NMR structure (Å) <sup>a</sup>	2.1 ± 0.1	1.7 ± 0.2	—
Intermolecular energy (kcal mol <sup>-1</sup> ) <sup>b</sup>	-392 ± 49	-443 ± 92	—
Buried surface area (Å <sup>2</sup> ) <sup>c</sup>	1453 ± 114	1676 ± 150	1365
Intermolecular Contacts <sup>d</sup>			
Number of H bonds/% of native H bond	9/40%	10/100%	5
Number of nonbonded contacts/% of native contact	11/21%	18/63%	19
Total number of intermolecular contacts/% of native contacts	20/25%	28/71%	24
% of total native contact present in at least one structure	58%	96%	

<sup>a</sup>The interface consists of residues 36–48, 66–82, 84–88, 92–98, and 139–143 for EIIA and residues 10–22 and 46–58 for HPr.

<sup>b</sup>The intermolecular energy consists of the sum of the van der Waals, the electrostatic and the AIR energy terms.

<sup>c</sup>Calculated with NACCESS (Hubbard and Thornton, 1993) using a 1.4 Å radius probe.

<sup>d</sup>Intermolecular contacts were analyzed with DIMPLLOT (Wallace et al., 1995) (see Experimental Procedures) and are reported if present in at least half of the analyzed structures. The percentages correspond to the percentage of native hydrogen bond or nonbonded contact in the NMR structure that are also present in at least half of the analyzed structures.

with unlabeled UbCH5B (Albert et al., 2002). The residues of CNOT4-N78 having the highest chemical shift perturbation upon binding to UbCH5B are Leu16, Cys17, Met18, Cys41, Asp48, Glu49, and Arg57. The mapping of these residues onto the CNOT4 RING finger NMR structure (PDB: 1E4U) (Hanzawa et al., 2001) reveals three distinct regions. The first region defines the shallow groove of the  $\alpha$  helix (residues 16–18) and the two other regions correspond to two zinc chelating loops (residues 48, 49, and 57).

In this study, we carried out the reciprocal experiment using <sup>15</sup>N-labeled UbCH5B and unlabeled CNOT4-N78 to identify the residues of UbCH5B involved in the interaction with the CNOT4 RING finger. The NMR titration was performed by increasing the UbCH5B/CNOT4 RING finger molar ratio up to a final 1:2 molar ratio. We analyzed the UbCH5B chemical shift perturbation upon binding to CNOT4-N78 and characterized the amino acids potentially involved in the interaction (Figure 2). The largest combined chemical shift differences (higher than 0.1 ppm) are observed in the first  $\alpha$  helix (Ala2,

Leu3, Arg5, Ile6, Glu9, Leu10, Asn11, and Asp12), the L1 loop connecting the third and fourth strand of the  $\beta$  sheet (residue Thr58, Asp59, Tyr60, and Lys63), and the L2 loop connecting the fourth  $\beta$  strand and the H2  $\alpha$  helix (residues Ser94, Ala96, Thr98, and Ile99). These residues define three distinct interacting regions of UbCH5B, which are located on one side of the molecule. This is consistent with previous data showing that CNOT4-N78 displays three distinct interacting regions upon binding to UbCH5B, which are localized around a hydrophobic cleft (Albert et al., 2002).

#### Ensemble Docking of the UbCH5B/CNOT4 RING Finger Complex

We used HADDOCK (Dominguez et al., 2003) to generate a structural model of the UbCH5B/CNOT4 RING finger domain based on the NMR titration data. A new feature that we added to HADDOCK consists of the possibility of starting from ensembles of structures instead of a single structure. The structure of a protein free in solution is usually different than when forming a complex with a partner. Even when very small structural rearrangements occur (that can be monitored by NMR or circular dichroism for example) the side chain orientation at the interface may be much more different. In HADDOCK, the proteins are treated as rigid bodies at the first stage of the docking. Since no flexibility is allowed at this stage, no side chains or loop rearrangement can occur which might lead to wrong initial orientations of the complex. Such orientations are generally not corrected during the subsequent HADDOCK semiflexible molecular dynamic refinement stages. A solution to overcome this problem can be to start from an ensemble of structures instead of a single molecule. An NMR ensemble of structures will reflect flexibility in loops and will show slight differences in side chain orientation especially for solvent-exposed residues. The different side chain and/or backbone orientations allow a better sampling of all conformational possibilities during the rigid body docking step. However, also in the case that an ensemble of NMR models or different X-ray structures or homology models are not available, an ensemble can be generated by applying a short molecular dynamics

Table 2. Active and Passive Residues of UbCH5B and CNOT4-N78

UbCH5B		CNOT4	
Active <sup>a</sup>	Passive <sup>b</sup>	Active	Passive
Leu3	Met1	Leu16	Glu13
Arg5	Lys4	Cys17	Pro15
Thr58	His7	Met18	Pro20
Asp59	Lys8	Glu19	His43
Lys63	Asp29	Phe40	Arg44
Ser94	Met30	Asp48	Thr47
Ala96	Phe31	Glu49	Pro54
Thr98	His55	Asn50	
	Phe62	Leu52	
	Lys66	Ala55	
	Gln92	Cys56	
	Pro95	Arg57	

<sup>a</sup>The active residues correspond to the residues having a significant NMR chemical shift perturbation during the NMR titration experiments and that are high solvent accessible.

<sup>b</sup>The passive residues correspond to all surface neighbors of the active residues that are solvent accessible.

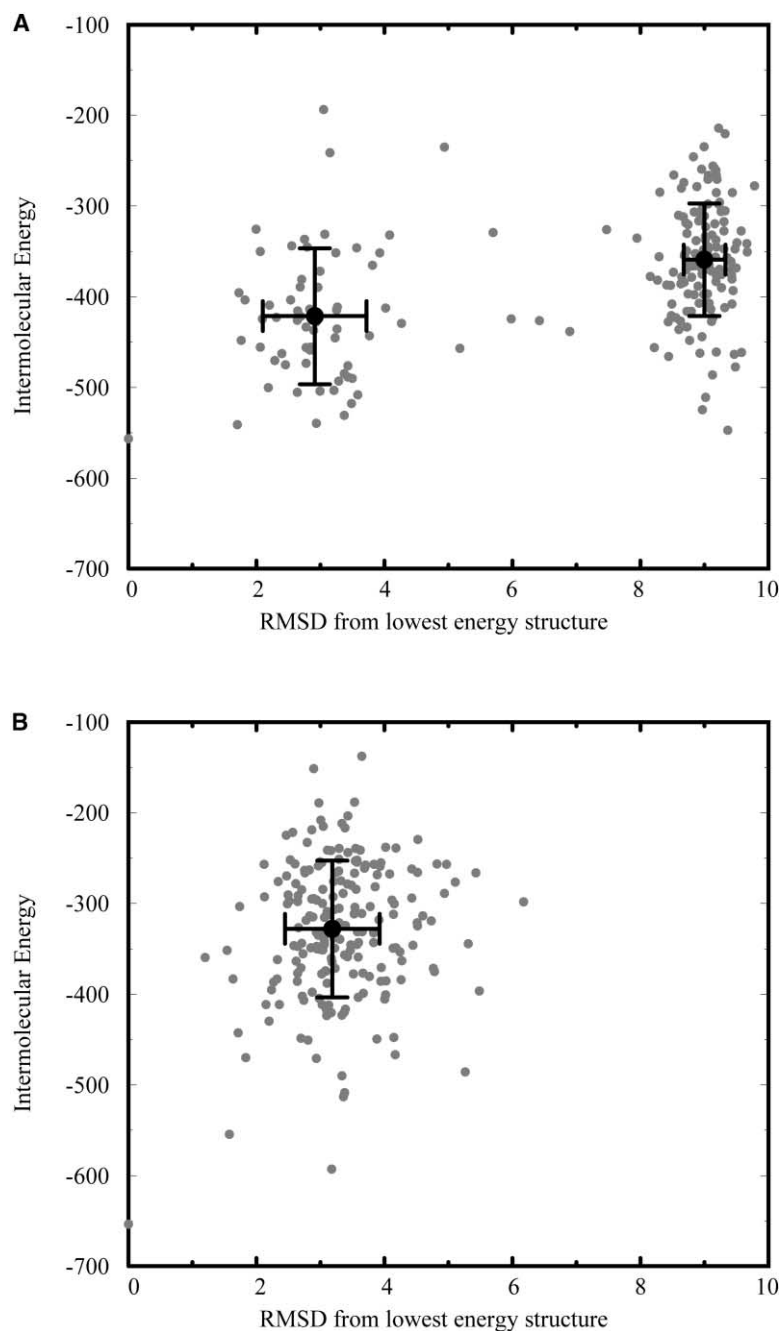


Figure 3. Docking Results of the Ubch5B/CNOT4 Complex

Plot of the intermolecular energy as a function of the rmsd from the lowest energy structure for the 200 calculated solutions (A) when using NMR chemical shift perturbation data only and (B) after incorporation of additional mutagenesis data. Black circles correspond to the averages of the clusters.

simulation. The different structures can then be extracted from the trajectory of the simulation.

The performance of ensemble docking was tested on the EIIA-HPr complex (Wang et al., 2000) starting from the X-ray structure of EIIA (Worthylake et al., 1991) and the 30 NMR structures of HPr (van Nuland et al., 1994; Worthylake et al., 1991). After the water refinement, only two clusters were obtained using a 1.5 Å cut-off for the ensemble docking instead of 14 when starting from single structures (Dominguez et al., 2003). The model obtained starting from an ensemble of structures is closer to the target complex than the single structure docking solution as can be seen from Table 1. In order

to get more insights into the validity of our docking approach, we also analyzed the intermolecular contacts present in our best models and compared them with the contacts present in the NMR structure. The analysis was performed using LIGPLOT (Wallace et al., 1995) on the 10 best solutions of the best cluster for the ensemble docking (this cluster contains 87 solutions) and on the 7 solutions of the best cluster for the original docking (see Table 1). The HADDOCK solution reproduced 100% of the hydrogen bonds and/or salt bridges found in the NMR structure and 63% on the nonbonded contacts (Table 1). Note that for the NMR structure, the analysis was based on a single structure, the deposited mini-

Table 3. Structural Statistics of the Ten Best UbchH5B/CNOT4 Model Structures

Backbone rmsd (Å) with respect to mean	
Flexible interface backbone <sup>a</sup>	1.70 ± 0.56
All backbone	2.69 ± 1.46
Number of ambiguous interaction restraints (AIRs)	
From UbchH5B	12
From CNOT4	8
Total AIRs	20
CNS intermolecular energies after water refinement <sup>b</sup>	
E <sub>vdw</sub> (kcal mol <sup>-1</sup> )	-54 ± 14
E <sub>elec</sub> (kcal mol <sup>-1</sup> )	-461 ± 75
Buried surface area (Å <sup>2</sup> ) <sup>c</sup>	1551 ± 117
Rmsd from idealized covalent geometry	
Bonds (Å)	0.003 ± 0.00
Angles (°)	0.43 ± 0.01
Impropers (°)	0.36 ± 0.01
Ramachandran analysis	
Residues in the favored region (%)	81.1 ± 2.4
Residues in additionally allowed regions (%)	16.8 ± 2.8
Residues in generously allowed regions (%)	1.3 ± 1.1
Residues in disallowed regions (%)	0.7 ± 0.3

Structural statistics of the ten best UbchH5B/CNOT4 model structures are based on structures obtained after flexible docking with HADDOCK followed by refinement in explicit water using ambiguous interaction restraints derived from chemical shift perturbation data (see Experimental Procedures).

<sup>a</sup>The flexible interface comprises segments M1-P18, V26-W33, T53-A68, and R90-L103 for UbchH5B, and V12-E22 and C38-P59 for CNOT4.

<sup>b</sup>The nonbonded energies were calculated with the OPLS parameters (Jorgensen and Tirado-rives, 1988) using a 8.5 Å cut-off.

<sup>c</sup>The buried surface area was calculated with CNS (Brunger et al., 1998) using a 1.4 Å radius water probe and 0.05 Å accuracy.

mized average, and no contact statistics could thus be obtained. This structure was also calculated in the absence of any attractive nonbonded energy term. Next to those “native” contacts, five additional intermolecular hydrogen bonds/salt bridges were detected in the HADDOCK models (Table 1).

For the docking of the UbchH5B/CNOT4 RING complex, 30 NMR structures of the CNOT4 RING domain deposited in the PDB (PDB: 1E4U) (Hanzawa et al., 2001) and 11 models of UbchH5B obtained during the molecular dynamic simulations (the initial homology model and 10 molecular dynamic structures taken at 0.5 ns intervals) (see Experimental Procedures) were used. Based on the NMR titration data, we first selected all residues having a combined chemical shift perturbation upon complex formation higher than 0.1 and 0.05 ppm for UbchH5B and CNOT4, respectively. The cut-off of 0.1 and 0.05 ppm was defined as all residues having a chemical shift perturbation higher than the average chemical shift perturbation along the sequence plus 1 standard deviation, in combination with a solvent accessibility criteria. In total, 12 and 8 active residues and 7 and 13 passive residues for CNOT4 and UbchH5B, respectively, were used to define 20 ambiguous interaction restraints (AIRs) to drive the docking process (Table 2) (see Experimental Procedures). After water refinement, two clusters were obtained (Figure 3A) containing 61 and 127 structures, respectively. The best 10 structures of these two clusters have average total interaction energies of  $-522 \pm 17$  and  $-487 \pm 29$  kcal·mol<sup>-1</sup>, AIR energies of  $2.23 \pm 2.07$  and  $1.28 \pm 0.72$  kcal·mol<sup>-1</sup> and buried surface areas of

$1388 \pm 81$  and  $1523 \pm 83$  Å<sup>2</sup>, respectively. The second cluster is the most populated, satisfies best the experimental restraints, and possesses the largest interface. Its total intermolecular energy is somewhat higher than the first cluster, due mainly to differences in electrostatic energies. In order to differentiate between these two clusters, we analyzed them in detail. The two clusters correspond to models with  $\sim 180^\circ$  rotation of CNOT4 around the intermolecular axis defined by the two proteins. The difficulty in distinguishing between them is due to the symmetry of the charge distribution at the interface. Two residues of CNOT4 showing a significant chemical shift perturbation upon complex formation are the amino acids Asp48 and Glu49. We thus investigated the hydrogen bond pattern in the two clusters. In the best solution of cluster 1, Asp48 and Glu49 of CNOT4 form salt bridges with the Lys4 and Lys8 of UbchH5B, while in the best solution of cluster 2, these two residues pair with Lys63 of UbchH5B. This 2-fold ambiguity in our models was solved by site-directed mutagenesis in combination with yeast two-hybrid assays, indicating that the Lys63 of UbchH5B interacts with Glu49 of CNOT4 (Winkler et al., 2004).

#### Ensemble Docking Based on NMR Chemical Shift Perturbation and Mutagenesis Data

We performed a new docking by defining, in addition to the previous ambiguous restraints derived from NMR chemical shift perturbation experiments, a restraint between any atom of Glu49 of CNOT4 and any atom of Lys63 of UbchH5B. Now, only one cluster could be detected containing 168 structures out of the 200 calculated when using a 2.5 Å rmsd (199 structures belong to this cluster when using a 3.0 Å rmsd) (Figure 3B). The complex is well defined with an average energy of the ten best structures of  $-515 \pm 65$  kcal·mol<sup>-1</sup>, and an average backbone rmsd of  $1.70 \pm 0.56$  Å at the interface (Table 3). The best solution of the cluster in terms of intermolecular energy ( $-653$  kcal·mol<sup>-1</sup>) is displayed in Figure 4 and is very similar to the best structure of the second cluster in the previous docking (total backbone rmsd of 1.2 Å while the total backbone rmsd between this model and the best model of the first cluster is 9.5 Å). In this cluster, salt bridges are found between Lys63 of UbchH5B with Asp48 and Glu49 of CNOT4, but also between Lys4 and Lys8 of UbchH5B with Glu13 of CNOT4, and Asp59 of UbchH5B with Arg44 of CNOT4 (Table 4). In addition to this salt bridges network, a number of van der Waals contacts occur at the interface between residues 1, 4, 5, and 8 of UbchH5B corresponding to the H1 helix and residues 15, 17, 18, 40, and 41 of CNOT4, between residues 62 of the L1 loop of UbchH5B and residues 44 and 45 of CNOT4, and finally between residues 92, 94, 95, and 96 of the L2 loop of UbchH5B and residues 49, 54, and 57 of CNOT4 (Table 4). Concerning the H1 helix, the first residue is not visible in the HSQC spectrum, residue 5 shows a significant perturbation in the NMR titration experiment and residues 4 and 8 have been shown to be involved in the interaction (Winkler et al., 2004). Concerning the loop L1, in addition to the salt bridges involving Asp59 and Lys63 of UbchH5B, both showing a significant perturbation, Phe62 is in van der Waals contact with residues

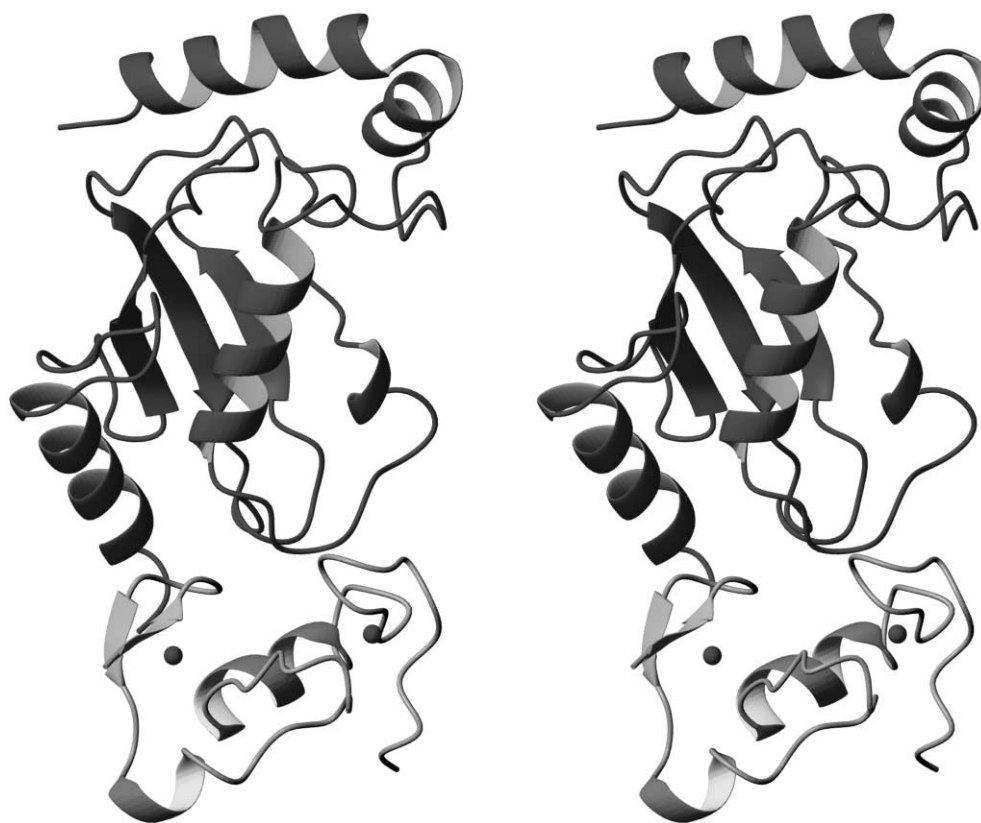


Figure 4. Stereoview of the Best Solution Generated by HADDOCK after Incorporation of Mutagenesis Data  
This figure has been generated with the program MOLMOL (Koradi et al., 1996)

of CNOT4. However, Phe62 does not show a significant perturbation. This could be due to the fact that all contacts between Phe62 and residues of CNOT4 involve the side chain aromatic ring and the perturbation is detected on the amide backbone atom. Finally, concerning loop L2, residues 94 and 96 show significant perturbation while Pro95 is not observed. On the CNOT4 side, all the residues involved in the van der Waals contacts show significant perturbation except for Arg44. The absence of perturbation for Arg44 is striking since this residue in our structural model is salt bridged to Asp59 of Ubch5B. The NMR titration data also showed that significant perturbation of the H1 helix of Ubch5B occurred up to residues Asp12. The structural model shows, however, that the last residue of this helix contacting CNOT4 is Lys8. This is consistent with the maximum length of the interacting area defined by the active and passive residues and by the shape of the molecules. The longest distance found in the interacting area of CNOT4 is between Glu19 and Arg57 and is about 27 Å. This distance fits the distance between Lys63 of Ubch5B and Lys8 in the H1 helix. Therefore, we assume that the perturbation observed for residues Glu9, Leu10, Asn11, and Asp12 of Ubch5B are due to an indirect effect of the binding to CNOT4.

#### Toward the Molecular Basis of the E2/E3 Specificity

Finally, we compared our structural model of the Ubch5B/CNOT4 complex with the X-ray structure of

c-Cbl/Ubch7 (Zheng et al., 2000). The two complexes are structurally homologous with a total backbone rmsd of 3.1 Å (Ubch5B/CNOT4 versus c-Cbl/Ubch7), and the orientation of the RING domain with respect to the E2 enzyme is similar in both complexes (Figure 5A). It has been shown, however, that the CNOT4 RING finger interacts specifically with Ubch5B and not with Ubch7 despite the fact that in both complexes the same regions of the E2s are involved in the interaction with the RING (Winkler et al., 2004). This suggests that although the three regions of Ubch5B and Ubch7 involved in the binding (helix H1, loops L1 and L2) are similar (Figure 2D), the binding properties must be different. It has already been reported that the L2 loop of E2 enzymes plays a role in the E2/E3 specificity (Martinez-Noel et al., 2001). In the Ubch7/c-Cbl crystal structure, the highly conserved P96 and A97 residues are involved in the binding. When comparing the residues of the L2 loop in Ubch5B and Ubch7, however, it can be noted that the other residues are not conserved between the two E2 enzymes: of these, Ser94, Thr98, and Ile99 of Ubch5B, which show significant NMR chemical shift perturbations, are replaced by two lysines (Lys96 and Lys100) and a threonine (Thr101) in Ubch7 (Figure 2D). In our model, we also observe the contacts involving the conserved Pro95 and Ala96. In addition, Ser94 makes a hydrogen bond with Arg57 of CNOT4 and a van der Waals contact with Pro54 (Table 4). No direct contact involving Thr98 or Ile99, however, could be detected in our model and, thus, we explain the observed chemical

Table 4. Intermolecular Contacts Statistics Calculated over the Ensemble of the Ten Best Structures of Cluster 1 for the Second HADDOCK Run

Interacting Residues		Hydrogen Bonds			Nonbonded Contacts	Occurrence
UbcH5B	CNOT4	M-M	S-S	M-S		
M1	C17	0	0	0	1	5
M1	P40	0	0	0	1	5
M1	C41	0	0	0	1	6
K4	E13	0	1	0	0	5
K4	M18	0	0	0	1	7
R5	P15	0	0	1	0	6
R5	M18	0	0	0	1	8
K8	E13	0	1	0	0	7
K8	M18	0	0	0	1	7
D59	R44	0	1	0	1	9
P62	R44	0	0	0	1	9
P62	I45	0	0	0	1	9
K63	D48	0	1	0	0	8
K63	E49	0	1	0	0	10
Q92	E49	0	1	0	0	5
Q92	R57	0	0	1	1	6
S94	P54	0	0	1	1	5
S94	R57	0	1	0	1	5
P95	E49	0	0	0	1	5
P95	P54	0	0	0	1	5
A96	P54	0	0	0	1	8

Intermolecular contacts were analyzed with DIMPLOT (Wallace et al., 1995) (see Experimental Procedures) and are reported if present in at least five of the ten best structures. The occurrence of main chain-main chain (M-M), side chain-side chain (S-S), and side chain-main chain (S-M) hydrogen bonds is reported. The number of occurrences of a given interaction over the ensemble of ten best structures is reported in the table.

shifts to an indirect effect of the complex formation. None of these nonconserved residues in UbchH7 are involved in direct contact with c-Cbl in the crystal structure. These results are in agreement with mutagenesis experiments in which a triple mutant of ubcM4 (K96S, T99L, K100T), which is highly homologous to UbchH7, was able to change the specificity from UbchM4 to UbchH5, demonstrating one or more of these residues are important for the specificity (Martinez-Noel et al., 2001).

A more detailed comparison of the UbchH5B/CNOT4 structural model with the X-ray structure of the c-Cbl/UbcH7 complex gives further insights into how the E2/E3 specificity occurs. Our NMR titration experiments suggest that the first  $\alpha$  helix of UbchH5B makes many direct contacts with the CNOT4 RING domain, whereas in the c-Cbl/UbcH7 complex, this helix provides only a minor contact with the c-Cbl RING finger domain through Arg5 and mainly interacts with the linker region located just N-terminal of the RING domain of c-Cbl (Zheng et al., 2000). Many residues of the first helix of UbchH5B show a significant chemical shift perturbation upon complex formation, and mutagenesis data showed that Lys4 and to a lesser extent Lys8 are critical residues for the binding to CNOT4-N78. The CNOT4 RING domain is located at the N terminus of the protein and does not possess this linker region. As a control, we performed a titration of  $^{15}\text{N}$ -UbchH5B with unlabeled CNOT4-N227 (the 227 N-terminal amino acids) containing the RRM (RNA recognition motif) domain to investigate whether another region of CNOT4 is involved in the interaction with the UbchH5B H1 helix. However, we did not observe any additional perturbation in the HSQC spectra (data not shown) indicating that, contrary to the c-Cbl/UbcH7

complex, CNOT4 interacts with UbchH5B only through its RING finger domain, and that the H1 helix of UbchH5B is interacting with the CNOT4 RING finger and not with another region of the protein. This is further supported by the fact that the structural model of the UbchH5B/CNOT4 complex shows several contacts between the H1 helix of UbchH5B and the RING domain of CNOT4 that are not present in the c-Cbl/UbcH7 complex (Figure 5B). Furthermore, the contacts that govern the binding of UbchH7 to c-Cbl involve mainly hydrophobic or uncharged residues making multiple van der Waals contacts. In the case of the UbchH5B/CNOT4 complex, however, many charged residues could be detected in the NMR titration experiments, suggesting that hydrogen bonds, salt bridges, and thus electrostatic interactions are important in the binding. In the c-Cbl/UbcH7 complex, indeed, residues Pro62 and Phe63 of the L1 loop make close contact with the c-Cbl RING domain. In contrast, our titration of UbchH5B shows significant chemical shift perturbations for Thr58, Asp59, Tyr60, and Lys63, while Phe62 is not affected and Pro61 cannot be observed. The presence of salt bridges in the UbchH5B/CNOT4 complex is further supported by the results of site-directed mutagenesis (Winkler et al., 2004). Though the residues Lys63 of UbchH5B and Glu49 of CNOT4 are conserved in UbchH7 (Lys64) and c-Cbl (Glu412), they do not form a contact in the crystal structure (Figure 5C).

Taken together, these results give insights into how two different E2/E3 complexes can interact in two distinct ways although their interaction regions are similar with rather high sequence homology. Our present work provides new insight into the origin of the specificity within a given E2/E3 complex in that it indicates that



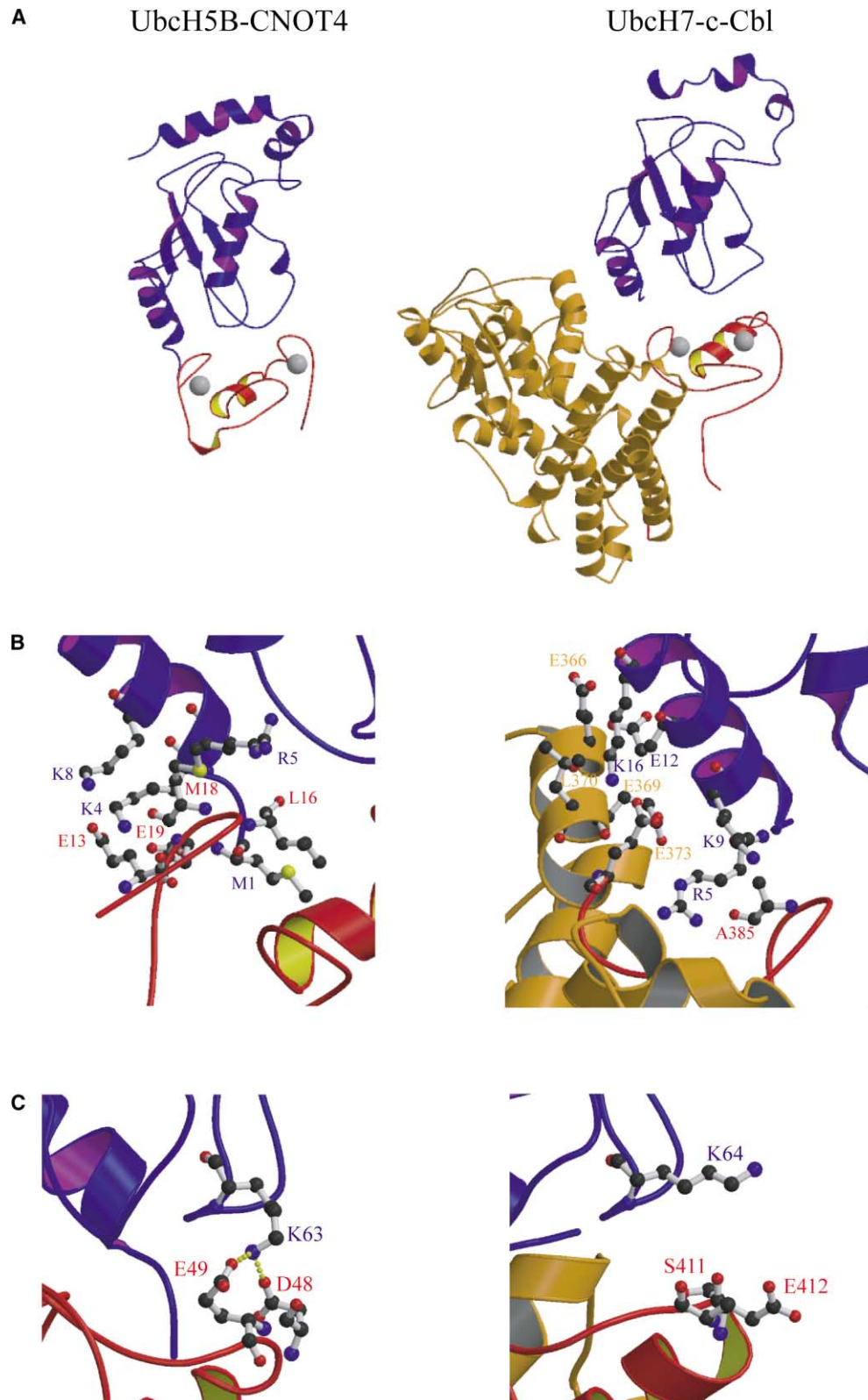


Figure 5. Comparison between the Ubch5B/CNOT4 Docking Model and the c-Cbl/UbcH7 Crystal Structure

(A) The orientation of the RING domain compared to the E2 enzyme is similar in both complexes. Ubch5B and Ubch7 are colored blue and purple, CNOT4 and c-Cbl RING domains are colored red and yellow, and the other domains of c-Cbl are colored orange.

(B) The helix  $\alpha 1$  of Ubch5B makes many contacts with the CNOT4 RING domain, whereas the helix  $\alpha 1$  of Ubch7 interact mainly with the linker region of c-Cbl. Residues 1, 4, 5, and 8 of Ubch5B and 5, 9, 12, and 16 of Ubch7 are labeled in blue. Residues 13, 16, 18, and 19 of CNOT4 and 385 of c-Cbl RING are labeled in red. Residues 366, 369, 370, and 373 corresponding to the linker region of c-Cbl are labeled in orange.

(C) In the L1 loop of Ubch5B, residue Lys63 interacts with CNOT4 Asp48 and Glu49, whereas the corresponding and conserved residue of Ubch7 (Lys64) is not in contact with c-Cbl. Figures have been generated with the programs Molscript (Kraulis, 1991) and Raster3D (Merritt and Murphy, 1994).

electrostatic interactions are of crucial importance. Other E2/E3 complexes will, however, need to be studied to fully understand the preference of ubiquitin-protein ligases for specific ubiquitin-conjugating enzymes.

## Experimental Procedures

### Recombinant Proteins Expression and Purification

The bacterial expression plasmids for Ubch5B, CNOT4-N78, and CNOT4-N227 have been described (Albert et al., 2002; Hanzawa et al., 2001). Overexpression of  $^{15}\text{N}$  and  $^{15}\text{N}/^{13}\text{C}$ -labeled GST-Ubch5B was accomplished by growing *Escherichia coli* BL21(DE3) containing the pGEX2T-Ubch5B plasmid in a synthetic medium (6.0 g/l  $\text{Na}_2\text{HPO}_4 \cdot 2\text{H}_2\text{O}$ , 3.0 g/l  $\text{KH}_2\text{PO}_4$ , 0.5 g/l NaCl, 1 mM  $\text{MgSO}_4$ , 20  $\mu\text{M}$   $\text{CaCl}_2$ , 36 nM  $\text{FeSO}_4 \cdot 7\text{H}_2\text{O}$ , 20  $\mu\text{M}$   $\text{ZnCl}_2$ , and 5 mg/l thiamine) containing 0.5 g/l  $^{15}\text{NH}_4\text{Cl}$  as the sole nitrogen source and either 4 g/l  $^{12}\text{C}$  glucose or 2.0 g/l  $^{13}\text{C}$  glucose as the only carbon source. Induction took place at  $A_{600} = 0.7\text{--}0.75$  by addition of 0.4 mM isopropyl- $\beta$ -thiogalactopyranoside (IPTG), and bacteria were grown 3 hr at 30°C and lysed in buffer LB (300 mM KCl, 50 mM Tris-HCl, pH 8.0, 2 mM EDTA, 0.1% Triton X-100, 20% sucrose) containing 1 mM dithiothreitol (DTT), 0.5 mM phenylmethylsulfonyl fluoride (PMSF), protease inhibitor cocktail (Roche), and 250  $\mu\text{g}/\text{ml}$  lysosome. After freeze thawing and sonication, lysates were centrifuged at 25 krpm in a SW40 rotor for 90 min at 4°C. Supernatant was bound to glutathione-agarose in LB buffer without sucrose, washed with buffer WB (150 mM KCl, 20 mM Kpi, pH 7.0, 10  $\mu\text{M}$   $\text{ZnCl}_2$ , protease inhibitors), and eluted with buffer WB plus 10 mM glutathione. The GST tag was cleaved by addition of 3 U of thrombin (Sigma) per milligram protein at 37°C for 3 hr. Thrombin was inactivated by addition of 0.5 mM PMSF (final concentration) and, subsequently, removed by batch binding to benzamidine-Sepharose6B (Amersham). The Ubch5B sample was concentrated using a stirred Amicon ultrafiltration cell (Millipore) and further purified by gel filtration chromatography using a Superdex75 16/60 column (Amersham) using WB buffer. Fractions containing Ubch5B were concentrated to a final concentration of 1 mM.

The expression and purification of unlabeled CNOT4-N78 and CNOT4-N227 were as described (Hanzawa et al., 2001). The samples were then dialyzed against NMR buffer (150 mM KCl, 20 mM Kpi, pH 7.0, 10  $\mu\text{M}$   $\text{ZnCl}_2$ ) and concentrated by ultrafiltration to a final concentration of 1 mM.

### Ubch5B Modeling

Ubch5B displays 90% homology and 80% identity with the yeast Ubc4 (PDB: 1QCQ) (Cook et al., 1993). We used Modeller4 (Sali and Blundell, 1993) to generate ten structural models of Ubch5B based on the structure of yeast Ubc4.

### Molecular Dynamic Simulation of Ubch5B

We selected the best model based on Procheck (Laskowski et al., 1993) analysis and applied a 5 ns molecular dynamic simulation in explicit solvent. PDB files were extracted from the trajectory every 0.5 ns so that, at the end of the simulation, 11 PDB files (the original plus 10 from the molecular dynamic) were available as starting structures for the docking. The molecular dynamic simulations were run with the GROMACS3.0 molecular dynamic package (Lindahl et al., 2001) using the GROMOS96 force field (Scott et al., 1999). The structure was solvated in a cubic box of SPC water (Berendsen et al., 1981) using a minimum distance of 14 Å between the protein and the box edges. After a first steepest descent energy minimization with positional restraints on the solute, one chloride counter ion ( $\text{Cl}^-$ ) was introduced to obtain an electro-neutralized system. A second energy minimization was performed, followed by five successive 20 ps molecular dynamic equilibration runs. During these, the position restraints force constant on the solute Kposre was decreased progressively (1000, 1000, 100, 10, 0  $\text{kJ}\cdot\text{mol}^{-1}\cdot\text{nm}^{-2}$ ). A 5 ns production run was then performed at constant temperature (300 K) and pressure (1 atm) with weak coupling (0.1 and 1  $\text{ps}^{-1}$ ) to reference T and P baths (Berendsen et al., 1984) using a 4 fs time step for the integration of the equations of motion. Nonbonded interactions were calculated using twin range cut-offs of 0.8 and

1.4 nm. Long-range electrostatic interactions beyond the cut-off were treated with the generalized reaction field model using a dielectric constant of 54 (Tironi et al., 1995). The LINCS algorithm (Hess et al., 1997) was used for bond length constraining in conjunction with dummy atoms for the aromatic rings and amino group in side chains (Feenstra et al., 1999) allowing the use of the longer integration time step of 4 fs.

### NMR Measurements

NMR experiments have been carried out at 300 K and pH 7.0 on a Bruker AVANCE600 and AVANCE700 equipped with a triple-resonance z-gradient probe.

For the backbone assignment of Ubch5B, 2D ( $^{15}\text{N}$ - $^1\text{H}$ )-HSQC, 2D ( $^{13}\text{C}$ - $^1\text{H}$ )-HSQC, 3D HNCQ, 3D HNCACB, and 3D CBCA(CO)NH were recorded. The side chain assignment was performed using 3D TOCSY-( $^{15}\text{N}$ - $^1\text{H}$ )-HSQC, 3D H(C)CH-TOCSY and 3D (H)CCH-TOCSY spectra (Sattler et al., 1999).

Concerning the chemical shift perturbation experiments, ( $^{15}\text{N}$ - $^1\text{H}$ )-HSQC spectra were recorded on ( $^{15}\text{N}$ - $^1\text{H}$ )-Ubch5B alone and in complex with different ratios of CNOT4-N78 (1:1/8 to 1:2). For all ( $^{15}\text{N}$ - $^1\text{H}$ )-HSQC spectra, 2048 points with a spectral width of 8012 Hz in the direct dimension and 512 points with a spectral width of 2200 Hz in the indirect dimension were recorded. The number of scans varied between 16 and 64 during the titration, and the relaxation delays were set to 1 s. All NMR spectra were processed using the NMRPipe package (Delaglio et al., 1995) and analyzed using the program NMRView (Johnson and Blevins, 1994).

### Docking

Docking of the Ubch5B/CNOT4 complex was performed using the software HADDOCK1.1 (Dominguez et al., 2003) in combination with CNS (Brunger et al., 1998) based on the chemical shift perturbation data observed for Ubch5B and for CNOT4 (Albert et al., 2002) upon complex formation. The starting structures for the docking were the 30 structures of CNOT4 deposited in the PDB (PDB: 1E4U) (Hanzawa et al., 2001) and the 11 models of Ubch5B generated during the molecular dynamic simulation. For the first docking, the active and passive residues defined for HADDOCK were chosen based on the chemical shift perturbation data and solvent accessibility (Table 2). We first selected all the residues having a combined chemical shift perturbation upon complex formation higher than 0.1 and 0.05 ppm for Ubch5B and CNOT4, respectively. We calculated the solvent accessibility using the program NACCESS (Hubbard and Thornton, 1993) over the ensemble of structures and selected as active residues all the amino acids showing an average relative solvent accessibility (plus standard deviation) higher than 50%. We then selected all surface neighbors amino acids having a high solvent accessibility (>50%) as passive residues. A 2 Å distance was used to define the ambiguous interaction restraints (AIR). Residues 1–18, 26–33, 53–68, and 90–103 of Ubch5B, and 12–22 and 38–59 of CNOT4 were defined as flexible. In the second docking, an additional restraint between any atoms of Lys63 of Ubch5B and any atoms of Glu49 of CNOT4 was defined based on mutagenesis experiments (Winkler et al., 2004). During the rigid body energy minimization, 1,320 structures were calculated (four calculations for each combination of starting structures). For each of the 1,320 combinations, 10 rigid body docking trials were performed and only the solution with lowest energy was kept amounting to a total of 13,200 rigid body minimization trials. The 200 best solutions based on the intermolecular energy were used for the semiflexible simulated annealing followed by a refinement in explicit water. Finally, the solutions were clustered using a 2.5 Å rmsd based on the pairwise backbone rmsd matrix after superposition on the backbone of Ubch5B.

### Analysis of the Intermolecular Contacts

Intermolecular contacts (hydrogen bonds and nonbonded contacts) were analyzed with DIMPLOT which is part of the LIGPLOT software (Wallace et al., 1995) using the default settings (3.9 Å heavy atoms distance cut-off for nonbonded contacts; 2.7 Å and 3.35 Å proton acceptor and donor-acceptor distance cut-offs, respectively, with minimum 90° angles (D-H-A, H-A-AA, D-A-AA) for hydrogen bonds (McDonald and Thornton, 1994).

## Acknowledgments

This investigation was supported by the Netherland Foundation for Chemical Research (NWO-CW) and the Netherland Organization for Scientific Research (NWO). This work was also supported by NWO "Jonge Chemici" and "Pionier" grants to A.M.J.J.B., and H.Th.M.T., respectively. C.D. was supported financially by the Center for Biomedical Genetics. The authors are grateful to Sandrine Jayne for critical reading of the manuscript.

Received: November 24, 2003

Revised: January 21, 2004

Accepted: January 24, 2004

Published: April 6, 2004

## References

- Albert, T.K., Hanzawa, H., Legtenberg, Y.I.A., de Ruwe, M.J., van den Heuvel, F.A.J., Collart, M.A., Boelens, R., and Timmers, H.T.M. (2002). Identification of a ubiquitin-protein ligase subunit within the CCR4-NOT transcription repressor complex. *EMBO J.* **21**, 355–364.
- Berendsen, H.C., Postma, J.P.N., van Gunsteren, W.F., and Hermans, J. (1981). Interaction models for water in relation to protein hydration. In *Intermolecular forces*, B. Pullman, ed. (Dordrecht, Reidel), pp. 331–342.
- Berendsen, H.J.C., Postma, J.P.M., van Gunsteren, W.F., DiNola, A., and Haak, J.R. (1984). Molecular dynamics with coupling to an external bath. *J. Chem. Phys.* **81**, 3684–3690.
- Bernier-Villamor, V., Sampson, D.A., Matunis, M.J., and Lima, C.D. (2002). Structural basis for E2-mediated SUMO conjugation revealed by a complex between ubiquitin-conjugating enzyme Ubc9 and RanGAP1. *Cell* **108**, 345–356.
- Brunger, A.T., Adams, P.D., Clore, G.M., DeLano, W.L., Gros, P., Grosse-Kunstleve, R.W., Jiang, J.S., Kuszewski, J., Nilges, M., Pannu, N.S., et al. (1998). Crystallography & NMR system: a new software suite for macromolecular structure determination. *Acta Crystallogr. D Biol. Crystallogr.* **54**, 905–921.
- Brzovic, P.S., Keefe, J.R., Nishikawa, H., Miyamoto, K., Fox, D., Ill, Fukuda, M., Ohta, T., and Kleit, R. (2003). Binding and recognition in the assembly of an active BRCA1/BARD1 ubiquitin-ligase complex. *Proc. Natl. Acad. Sci. USA* **100**, 5646–5651.
- Collart, M.A. (2003). Global control of gene expression in yeast by the Ccr4-Not complex. *Gene* **313**, 1–16.
- Cook, W.J., Jeffrey, L.C., Sullivan, M.L., and Vierstra, R.D. (1992). Three-dimensional structure of a ubiquitin-conjugating enzyme (E2). *J. Biol. Chem.* **267**, 15116–15121.
- Cook, W.J., Jeffrey, L.C., Xu, Y., and Chau, V. (1993). Tertiary structures of class I ubiquitin-conjugating enzymes are highly conserved: crystal structure of yeast Ubc4. *Biochemistry* **32**, 13809–13817.
- Cook, W.J., Martin, P.D., Edwards, B.F.P., Yamazaki, R.K., and Chau, V. (1997). Crystal structure of a class I ubiquitin conjugating enzyme (Ubc7) from *Saccharomyces cerevisiae* at 2.9 angstroms resolution. *Biochemistry* **36**, 1621–1627.
- Cornilescu, G., Delaglio, F., and Bax, A. (1999). Protein backbone angle restraints from searching a database for chemical shift and sequence homology. *J. Biomol. NMR* **13**, 289–302.
- Delaglio, F., Grzesiek, S., Vuister, G.W., Zhu, G., Pfeifer, J., and Bax, A. (1995). NMRPipe: a multidimensional spectral processing system based on UNIX pipes. *J. Biomol. NMR* **6**, 277–293.
- Denis, C.L., and Chen, J. (2003). The CCR4-NOT complex plays diverse roles in mRNA metabolism. *Prog. Nucleic Acid Res. Mol. Biol.* **73**, 221–250.
- Dominguez, C., Boelens, R., and Bonvin, A.M.J.J. (2003). HADDOCK: a protein-protein docking approach based on biochemical or biophysical information. *J. Am. Chem. Soc.* **125**, 1731–1737.
- Farrow, N.A., Archer, S.J., Wu, Z.J., Camac, D.M., Parsons, T., Rolfe, M., and Domaille, P.J. (2000). Backbone resonance assignment of human UBC4. *J. Biomol. NMR* **18**, 363–364.
- Feenstra, K.A., Hess, B., and Berendsen, H.J.C. (1999). Improving efficiency of large time-scale molecular dynamics simulations of hydrogen-rich systems. *J. Comput. Chem.* **20**, 786–798.
- Glickman, M.H., and Ciechanover, A. (2002). The ubiquitin-proteasome proteolytic pathway: destruction for the sake of construction. *Physiol. Rev.* **82**, 373–428.
- Hamilton, K.S., Ellison, M.J., Barber, K.R., Williams, R.S., Huzil, J.T., McKenna, S., Ptak, C., Glover, M., and Shaw, G.S. (2001). Structure of a conjugating enzyme-ubiquitin thiolester intermediate reveals a novel role for the ubiquitin tail. *Structure (Camb)* **9**, 897–904.
- Hanzawa, H., de Ruwe, M.J., Albert, T.K., van Der Vliet, P.C., Timmers, H.T.M., and Boelens, R. (2001). The structure of the C4C4 ring finger of human NOT4 reveals features distinct from those of C3HC4 RING fingers. *J. Biol. Chem.* **276**, 10185–10190.
- Hess, B., Bekker, H., Berendsen, H.J.C., and Fraaije, J. (1997). LINCS: a linear constraint solver for molecular simulations. *J. Comput. Chem.* **18**, 1463–1472.
- Huang, L., Kinnucan, E., Wang, G., Beaudenon, S., Howley, P.M., Huibregtse, J.M., and Pavletich, N.P. (1999). Structure of an E6AP-UbcH7 complex: insights into ubiquitination by the E2-E3 enzyme cascade. *Science* **286**, 1321–1326.
- Hubbard, S.J., and Thornton, J.M. (1993). NACCESS. Department of Biochemistry and Molecular Biology, University College London, UK.
- Jiang, F., and Basavappa, R. (1999). Crystal structure of the cyclin-specific ubiquitin-conjugating enzyme from clam, E2-C, at 2.0 Å resolution. *Biochemistry* **38**, 6471–6478.
- Johnson, B.A., and Blevins, R.A. (1994). NMRView: a computer program for the visualization and analysis of NMR data. *J. Biomol. NMR* **4**, 603–614.
- Jorgensen, W.L., and Tirado-rives, J. (1988). The OPLS potential functions for proteins. Energy minimizations for crystals of cyclin peptides and crambin. *J. Am. Chem. Soc.* **110**, 1657–1666.
- Koradi, R., Billeter, M., and Wuthrich, K. (1996). MOLMOL: a program for display and analysis of macromolecular structures. *J. Mol. Graph.* **14**, 51–55, 29–32.
- Kraulis, P.J. (1991). MOLSCRIPT: a program to produce both detailed and schematic plots of protein structures. *J. Appl. Crystallogr.* **24**, 946–950.
- Laskowski, R., MacArthur, M., Moss, D., and Thornton, J. (1993). PROCHECK: a program to check the stereochemical quality of protein structures. *J. Appl. Crystallogr.* **26**, 283–291.
- Lin, Y., Hwang, W.C., and Basavappa, R. (2002). Structural and functional analysis of the human mitotic-specific ubiquitin-conjugating enzyme, UbcH10. *J. Biol. Chem.* **277**, 21913–21921.
- Lindahl, E., Hess, B., and van der Spoel, D. (2001). GROMACS3.0: a package for molecular simulation and trajectory analysis. *J. Mol. Model.* **7**, 306–317.
- Martinez-Noel, G., Muller, U., and Harbers, K. (2001). Identification of molecular determinants required for interaction of ubiquitin-conjugating enzymes and RING finger proteins. *Eur. J. Biochem.* **268**, 5912–5919.
- McDonald, I.K., and Thornton, J.M. (1994). Satisfying hydrogen bonding potential in proteins. *J. Mol. Biol.* **238**, 777–793.
- Meritt, E.A., and Murphy, M.E.P. (1994). Raster3D version 2.0: a program for photorealistic molecular graphics. *Acta Crystallogr. D50*, 869–873.
- Miura, T., Klaus, W., Ross, A., Guntert, P., and Senn, H. (2002). The NMR structure of the class I human ubiquitin-conjugating enzyme 2b. *J. Biomol. NMR* **22**, 89–92.
- Moraes, T.F., Edwards, R.A., McKenna, S., Pastushok, L., Xiao, W., Glover, J.N., and Ellison, M.J. (2001). Crystal structure of the human ubiquitin conjugating enzyme complex, hMms2-hUbc13. *Nat. Struct. Biol.* **8**, 669–673.
- Pickart, C.M. (2001). Mechanisms underlying ubiquitination. *Annu. Rev. Biochem.* **70**, 503–533.
- Sali, A., and Blundell, T.L. (1993). Comparative protein modelling by satisfaction of spatial restraints. *J. Mol. Biol.* **234**, 779–815.
- Sattler, M., Schleucher, J., and Griesinger, C. (1999). Heteronuclear

multidimensional NMR experiments for the structure determination of proteins in solution employing pulsed field gradients. *Prog. NMR Spec.* 34, 93–158.

Scott, W.R.P., Hunenberger, P.H., Tironi, I.G., Mark, A.E., Billeter, S.R., Fennen, J., Torda, A.E., Huber, T., Kruger, P., and van Gunsteren, W.F. (1999). THE GROMOS biomolecular simulation program package. *J. Phys. Chem.* 103, 3596–3607.

Tironi, I.G., Sperb, R., Smith, P.E., and van Gunsteren, W.F. (1995). A generalized reaction field method for molecular dynamics simulations. *J. Chem. Phys.* 102, 5451–5459.

Tong, H., Hateboer, G., Perrakis, A., Bernards, R., and Sixma, T.K. (1997). Crystal structure of murine/human Ubc9 provides insight into the variability of the ubiquitin-conjugating system. *J. Biol. Chem.* 272, 21381–21387.

VanDemark, A.P., Hofmann, R.M., Tsui, C., Pickart, C.M., and Wolberger, C. (2001). Molecular insights into polyubiquitin chain assembly: crystal structure of the Mms2/Ubc13 heterodimer. *Cell* 105, 711–720.

van Nuland, N.A., Hangyi, I.W., van Schaik, R.C., Berendsen, H.J., van Gunsteren, W.F., Scheek, R.M., and Robillard, G.T. (1994). The high-resolution structure of the histidine-containing phosphocarrier protein HPr from *Escherichia coli* determined by restrained molecular dynamics from nuclear magnetic resonance nuclear Overhauser effect data. *J. Mol. Biol.* 237, 544–559.

Wallace, A.C., Laskowski, R.A., and Thornton, J.M. (1995). LIGPLOT: a program to generate schematic diagrams of protein-ligand interactions. *Protein Eng.* 8, 127–134.

Wang, G., Louis, J.M., Sondej, M., Seok, Y.J., Peterkofsky, A., and Clore, G.M. (2000). Solution structure of the phosphoryl transfer complex between the signal transducing proteins HPr and IIA(glucose) of the *Escherichia coli* phosphoenolpyruvate:sugar phosphotransferase system. *EMBO J.* 19, 5635–5649.

Weissman, A.M. (2001). Themes and variations on ubiquitylation. *Nat. Rev. Mol. Cell Biol.* 2, 169–178.

Winkler, G.S., Albert, T.K., Dominguez, C., Legtenberg, Y.I., Boelens, R., and Timmers, H.T.M. (2004). An altered-specificity ubiquitin-conjugating enzyme/ubiquitin protein ligase pair. *J. Mol. Biol.* 337, 157–165.

Worthylake, D., Meadow, N.D., Roseman, S., Liao, D.I., Herzberg, O., and Remington, S.J. (1991). Three-dimensional structure of the *Escherichia coli* phosphocarrier protein IIIgIc. *Proc. Natl. Acad. Sci. USA* 88, 10382–10386.

Worthylake, D.K., Prakash, S., Prakash, L., and Hill, C.P. (1998). Crystal structure of the *Saccharomyces cerevisiae* ubiquitin-conjugating enzyme Rad6 at 2.6 Å resolution. *J. Biol. Chem.* 273, 6271–6276.

Zheng, N., Wang, P., Jeffrey, P.D., and Pavletich, N.P. (2000). Structure of a c-Cbl-UbcH7 complex: RING domain function in ubiquitin-protein ligases. *Cell* 102, 533–539.

#### Accession Numbers

The coordinates of the five best structural models of the UbcH5B/CNOT4 complex have been deposited in the Protein Data Bank (accession code 1UR6) together with the AIR restraints.